

Radiative Transfer in Exoplanet Atmospheres

Rion Glenn Nazareth¹*

¹*School of Physical Sciences, National Institute of Science Education and Research*

23rd August 2023

ABSTRACT

The retrieval of the chemical composition and physical parameters of exoplanets is vital for potentially detecting biosignatures in them. The stellar light which passes through the planet has information about the constituents of the planet. Through radiative transfer, we can probe into the behaviour of light when it interacts with the exoplanet atmosphere. Several theoretical models exist which take into account absorption, emission and scattering to simulate photon interactions in the planetary atmosphere. In this paper, I review a few of the assumptions that go into building one such theoretical model known as ATMO and summarise the techniques used to compare it to observational data by demonstrating the detection of H_2O and CO_2 in WASP-39b, a hot-Jupiter exoplanet, using ATMO. I find that the techniques used to retrieve the parameters heavily rely on statistical tools. However, even though this makes the predictions robust, there can be a degeneracy in the fitted parameters where two different parameter space elements could give us identical spectra.

Key words: radiative transfer, biosignatures, spectra, ATMO

1 INTRODUCTION

The study of exoplanet atmospheres is mainly motivated by the search for the presence of biosignatures on them. As it is impossible to probe the interiors of exoplanets due to limits in our observational instruments, the atmosphere of the exoplanet is the next best place to look for biosignatures.

This emitted light had hints of the molecular abundances and physical characteristics of the exoplanet atmosphere Seager & Deming (2010). To better understand this characteristic emission, we use radiative transfer. As the number of transiting exoplanets discovered grew, the need for building more sophisticated radiative transfer retrieval models grew along with it. With the James Webb Space Telescope (JWST), we can probe deeper into exoplanet atmospheres than ever before. In this work, we first illustrate the methods used to obtain the data. Then, we describe the physics of building a radiative transfer model by choosing one such radiative transfer model known as ATMO. Drummond et al. (2016). Using ATMO, we demonstrate how the molecular abundances are retrieved using statistical techniques. In addition, the detection of H_2O using the Hubble Space Telescope data Wakeford et al. (2017) and CO_2 using the recent JWST data The JWST Transiting Exoplanet Community Early Release Science Team et al. (2022) is also demonstrated. We then briefly discuss the limitations of present-day radiative transfer models. This work is important because the literature about the physics involved in modern radiative transfer codes is either too complicated or non-existent. This work also gives a feel for how radiative transfer codes have improved throughout the years

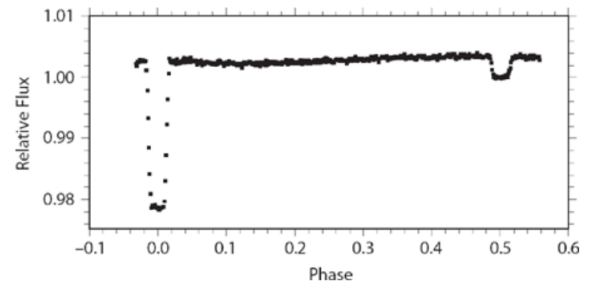


Figure 1. Dip in the light curve. Source: Seager & Deming (2010)

2 METHODS

2.1 Observational techniques

The main methods include the radial velocity and the transit method. In the transit method, variation in the flux of the star is measured as the planet passes through the star. This method depends on the fact that the orbital plane of the system is aligned with the line of sight. As the planet transits its host star, there is a dip in the light curve ¹ as shown in 1.

A transiting exoplanet has two transits: Primary transit and a secondary eclipse. The primary transit occurs when the planet is in the line of sight of the host star. The secondary eclipse occurs when the planet is just about to go behind its host star, as shown in 2. The main principle used

* riong.nazareth@niser.ac.in

¹ A light curve is the variation of the relative flux of the system as the planet transits its host star

wavelength dependent as we want the planet's spectrum. Scattering is incorporated into the source function as

$$J_\lambda(\mu, \phi) = (1 - \tilde{\omega})B(T, \lambda) + \frac{\tilde{\omega}}{4\pi} \int_0^{2\pi} \int_{-1}^1 p(\mu, \phi; \mu', \phi') I_\lambda((\mu', \phi')) d\mu' d\phi' \quad (3)$$

Where $B(T, \lambda)$ is the black-body function. $\tilde{\omega}$ is called the single-scatter albedo. It is assumed that the thermal emission from the atmosphere is negligible, and hence the surface of the planet is approximated as a black body since it is optically thick. $\tilde{\omega}$ also gives us the degree up to which scattering takes place in the atmosphere with $\tilde{\omega} = 0$ corresponding to no scattering and $\tilde{\omega} = 1$ corresponding to all scattering. $p(\mu, \phi; \mu', \phi')$ is called the scattering phase function and can be interpreted as the probability that the photon arrives in direction (μ, ϕ) from the direction (μ', ϕ') . If we take into account energy conservation in each scattering event, we can see that the phase function is normalised to 1.

Let $\cos \Theta = \Omega \cdot \Omega'$ where Ω is the direction of incidence and Ω' is the scattered direction. We can now assume that the phase function is only a function of $\cos \Theta$. Thus we get the normalisation condition

$$\frac{1}{2} \int_{-1}^1 p(\cos \Theta) d \cos \Theta = 1 \quad (5)$$

Now the probability of forward scatter is never equal to the probability of backwards scatter. Hence there is an asymmetry introduced in the problem. The asymmetry parameter is defined as

$$g \equiv \frac{1}{4\pi} \int_{4\pi} p(\cos \Theta) \cos \Theta d\omega \quad (6)$$

This parameter gives us a sense of the average value of $\cos \Theta$ for multiple photons. A phase function widely used in radiative transfer codes is the Henyey-Greenstein phase function.

$$p_{\text{HG}}(\cos \Theta) = \frac{1 - g^2}{(1 + g^2 - 2g \cos \Theta)^{3/2}} \quad (7)$$

2.2.2 Case Study: ATMO

ATMO is a code which solves the 1-D radiative transfer equation assuming plane parallel geometry and isotropic scattering, i.e. ($p \equiv 1$) [Drummond et al. \(2016\)](#). Since radiative transfer codes are solved numerically with techniques such as Gauss Siedel, we need to choose a spectral resolution up to which we want the emission spectra. It was first used to simulate brown dwarfs. Later on, it was modified for simulating the exoplanets with high levels of irradiation such as hot Jupiters. Since this model assumes isotropic scattering, p is set to 1 in (3) and the equation is solved using the following iterative equation

$$I_{\text{rad}}(\lambda) = I_{\text{rad}}^0(\lambda) e^{-|(\tau_\lambda/\mu)|} + \int_0^{\tau_\lambda/\mu} J_\lambda(\mu, \phi) e^{\tau' - |(\tau_\lambda/\mu)|} d\tau' \quad (8)$$

This is known as the line-by-line (LBL) approach [Petty \(Goy\)](#). This method is computationally intensive and is not ideal to generate spectra especially while using the retrieval model where millions of spectra need to be generated to obtain the best fit model. Hence correlated-k approximation is used which agrees with the LBL approach⁴.

In this analysis, we assumed that scattering occurs only

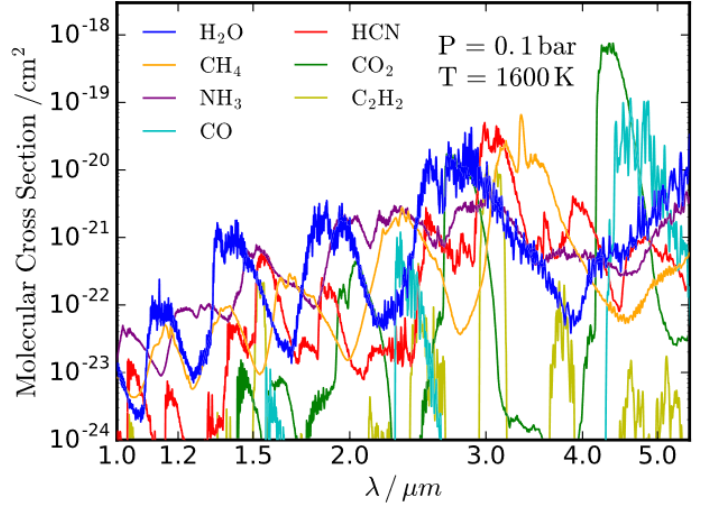


Figure 4. Molecular absorption cross section at $P = 0.1$ bar and $T = 1600$ K

due to a single gas species. To incorporate multi-gas Rayleigh scattering, we write the single scatter albedo in (3) as

$$\tilde{\omega} = \frac{\kappa_{\text{scat}}}{\kappa_{\text{scat}} + \kappa_{\text{abs}}} \quad (9)$$

Where κ_{scat} is known as the scattering opacity which is obtained by dividing the scattering cross section σ_{scat} by the weight of the species which scatters the photon. κ_{abs} is the absorption opacity which is obtained by dividing the absorption cross section σ_{abs} by the weight of the species which scatters the photon. The absorption cross-sections are calculated from the Einstein coefficients corresponding to different molecules. In addition to this, the effects of Pressure Broadening and Doppler Broadening are also taken into account. The molecular absorption cross sections for a few of the gas species considered in [Gandhi & Madhusudhan \(2018\)](#) is shown in 4. For multi-gas scattering, we also need to take into account that different gases change the photon polarisation in a different way when they scatter. To take this into account the scattering cross section is chosen as follows from [Liou \(2002\)](#).

$$\sigma_{\text{scat}}(\lambda) = \frac{8\pi^3(m_r^2 - 1)^2}{3\lambda^4 N_s^2} f(\delta) \quad (10)$$

Where λ is the wavelength, m_r is the refractive index⁵ of the species of gas, and N_s is the number density of the gas in the layer. $f(\delta)$ is the factor which takes into account the anisotropic properties of the species. It is given by $\frac{6+3\delta}{6-7\delta}$ where δ is the depolarisation factor⁶. The value depends on the species of gas chosen.

For simplicity, it is assumed that the elements found in the planet and its host star are the same. Hence the elemental abundances are varied using two parameters: the Carbon to Oxygen (C/O) ratio and the metallicity⁷ of the planet. This approximation reduces the parameter space by a significant amount.

⁵ real part

⁶ typical value of 0.035

⁷ mass fraction of the elements heavier than helium

⁴ We will not get into this technique in this paper.

2.2.3 Incorporation of haze

One major difference between radiative transfer in planets and stars is the presence of haze which are small aerosol particles which scatter light. The effect due to haze is represented by a haze enhancement factor which is a parameterised factor multiplied by the net scattering cross section due to all the gases⁸.

2.2.4 Incorporation of clouds

Clouds contain different types of aerosol particles. Since the types of aerosols in exoplanet atmospheres are challenging to constrain, the scattering opacity of clouds is just taken to be the scattering opacity of hydrogen molecule multiplied by a factor α_{cloud} which is known as the cloudiness factor. The total scattering opacity is given by

$$\kappa_{scat}^t = \kappa_{scat} + \alpha_{cloud} \kappa_{H_2} \quad (11)$$

where κ_{scat}^t is the total scattering opacity and κ_{scat} is the scattering opacity from all the molecules. κ_{H_2} is the scattering opacity of hydrogen.

3 RESULTS AND DISCUSSIONS

The forward model is used to simulate the transmission spectra of WASP-121b which is a hot-Jupiter. The C/O ratios and metallicities are obtained by parametrising the values of the T-P profiles and mole fraction variation with pressure for different species. Figure 5 shows the variation of the spectra with the C/O ratio whereas 6 shows the metallicity variation

3.1 Choosing the parameters

Once the forward model is optimised, it is used by the retrieval model. A grid of parameters such as optical depth, C/O ratios, Metallicity etc. is chosen. The retrieval model iterates throughout the entire parameter space and the best-fit model is chosen by calculating the χ^2 values compared to observations. We analyse the retrieval of WASP-39b which is a "hot Jupiter" exoplanet with a mass similar to Saturn to demonstrate the detection of water and more recently CO_2 . In 7 the contours of the parameters are plotted for WASP-39b. The colours indicate the confidence intervals obtained while comparing it to HST data. From 7 we can see that for $\alpha_{haze} = 10$ and $\alpha_{cloud} = 0.2$ the model shows minimum deviation from the data. Similarly, the values for the C/O ratio and metallicity are found to be 0.56 and 1 times solar metallicity respectively. We discuss the application of retrieval models to detect water and CO_2 .

3.2 Detection of Water from HST data

This analysis is taken from Wakeford et al. (2017). In plot 8, the complete transmission spectra of WASP-39b are shown. To fit the spectra, ATMO was run 6272 times with the value of parameters changing. The best fit model was found to have

⁸ This is just the sum of scattering due to individual molecules since it is additive Petty (Goy)

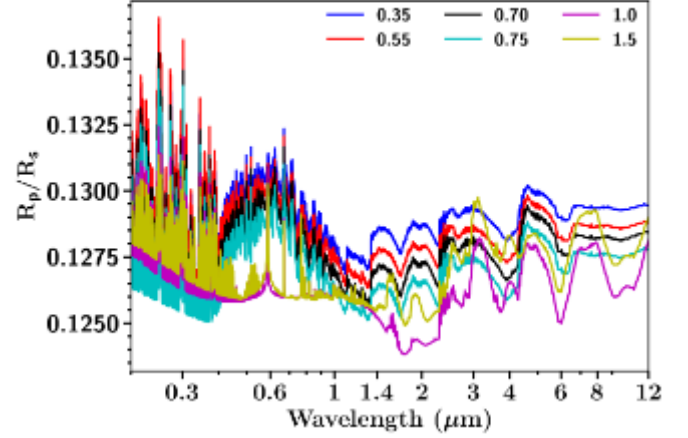


Figure 5. Variation of the transmission spectra with the C/O ratio in ATMO. Source: Goyal et al. (2020)

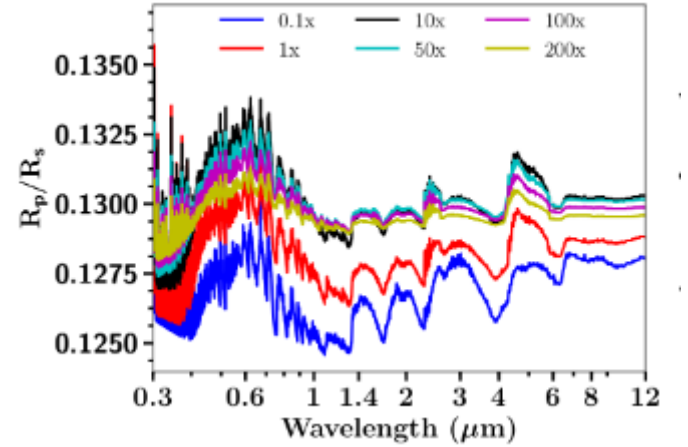


Figure 6. Variation of the transmission spectra with the metallicity values relative to the solar metallicity Source: Goyal et al. (2020)

$\alpha_{haze} = 150$ and $\alpha_{cloud} = 0.2$ the model shows minimum deviation from the data. Similarly, the values for the C/O ratio and metallicity are found to be 0.15 and 100 times solar metallicity respectively. These values are significantly different from previous estimates. As we can see in 8 the absorption features due to H_2O are clearly visible. This can also be confirmed by the high metallicity of the best-fit model. However, as we can see in 8 there isn't enough evidence to make any claims about the abundance of CO_2 . This was improved with the advent of JWST.

3.3 Detection of CO_2 from JWST data

This analysis is taken from The JWST Transiting Exoplanet Community Early Release Science Team et al. (2022). In 9, CO_2 was identified to be present in the atmosphere of the exoplanet WASP-39b. The black dots with error-bars is the reduced data obtained using the FIREFLY pipeline on the JWST data release.

In the top panel, the transit depth is plotted against the wavelength for the planet WASP-39b. The transit depth

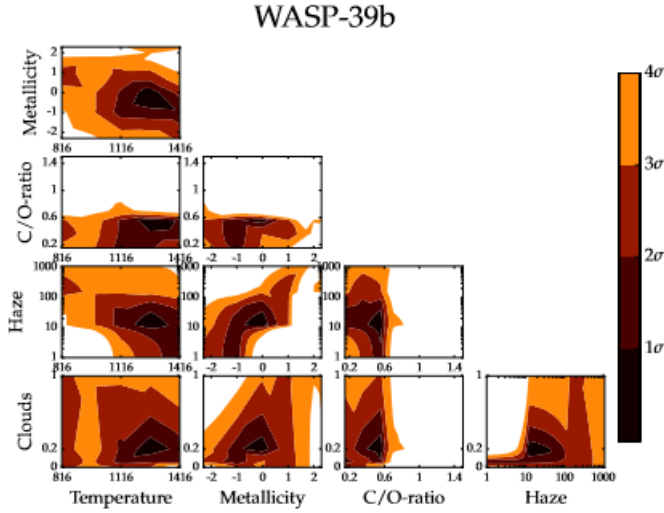


Figure 7. χ^2 contour for a range parameters(log-scaled). Colours indicate confidence intervals. Source: Goyal et al. (2020)

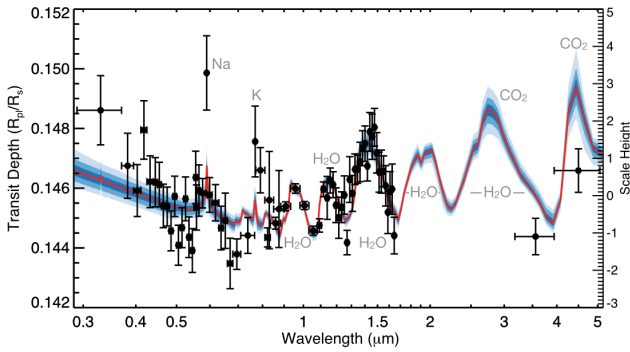


Figure 8. Transmission spectra obtained from HST STIS and WFC3, Spitzer IRAC, and VLT FORS2. ATMO retrieval model is fitted to the data

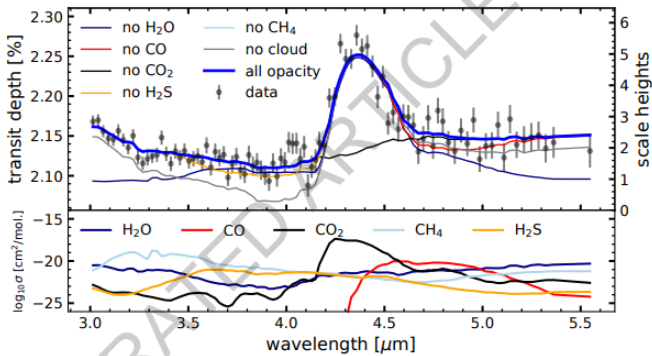


Figure 9. Transit depth(%) vs Wavelength(μm) data and model. Source: The JWST Transiting Exoplanet Community Early Release Science Team et al. (2022)

corresponding to different wavelengths differ based on the amount of light which is emitted or absorbed for each wavelength in the atmosphere of the exoplanet.

Using the absorption cross sections (shown in the bottom panel), the model finds the transit depth by solving the radiative transfer equation for each wavelength. Various parameters such as stellar metallicity, carbon-to-oxygen ratio, and cloud opacity are varied in the model (while solving the radiative transfer equation) and the best-fit model is chosen using the chi-square goodness of fit test.

The value of χ^2/N_{data} obtained using the best-fit model is 1.39 for ATMO. This led the authors to conclude that the assumptions made broadly capture the important physics and chemistry in WASP-39b's atmosphere. The optimal model resulting from this process has metallicity = 10 times solar metallicity, C/O = 0.7, $\alpha_{haze} = 10$ and $\alpha_{cloud} = 5$

We can see through the black curve in the plot that when the effect of CO_2 is neglected in the model, no absorption feature is seen in the transit depth in the CO_2 absorption regime (4.1 - 4.6 μm). This further strengthens our claim of the presence of CO in the atmosphere. We can also see a significant rise in transit depth at 3.6 μm due to the presence of water vapour.

4 CONCLUSIONS

The ways in which the emission and transmission spectra are obtained for a planet are described. The physics that goes into building radiative transfer models is explained by demonstrating the use of the ATMO forward model in obtaining the transmission spectra. The ATMO forward model is then used to retrieve the atmospheric parameters such as C/O ratios and metallicities.

In order to simulate the spectra which best match the observations, We need to run millions of simulations exhausting the whole parameter space. Madhusudhan & Seager (2009). This makes the model computationally intensive. In order to reduce the computational cost, statistical tools such as the correlated-k technique are used. These techniques are not discussed in this work.

Even though the methods used in determining the atmospheric parameters are sophisticated, there can be degeneracy in the estimates. This is evident if we compare 3.1 and 3.2. The metallicity estimates in the two cases for the same planet differ by a factor of 100. This mainly arises due to poor-quality data. This makes the models heavily dependent on the data. Hence the exoplanet committee checks for self-consistency by comparing models built by different authors.

As we need to run multiple models for retrieval, the effect of 3-D effects is neglected due to limitations in computing power. Also, the incorporation of clouds and haze is done using a preliminary model which can be further improved by better knowledge of the aerosols found in the interior atmospheres of exoplanets.

References

- Drummond B., Tremblin P., Baraffe I., Amundsen D. S., Mayne N. J., Venot O., Goyal J., 2016, *Astronomy and Astrophysics*, 594, A69
- Fišák J., Krtićka J., Munzar D., Kubát J., 2016, *Astronomy & Astrophysics*, 590, A95
- Gandhi S., Madhusudhan N., 2018, *Monthly Notices of the Royal Astronomical Society*, 474, 271–288

- Goyal J. M., et al., 2020, Monthly Notices of the Royal Astronomical Society
- Haswell C. A., 2010, Transiting exoplanets. Cambridge University Press, Cambridge
- Korkin S., Sayer A. M., Ibrahim A., Lyapustin A., 2022, Computer Physics Communications, 271, 108198
- Liou K.-N., 2002, An introduction to atmospheric radiation. Vol. 84, Elsevier
- Madhusudhan N., Seager S., 2009, *ApJ*, **707**, 24
- Petty G. W., 2006, A first course in atmospheric radiation, 2nd edn. Sundog Pub, Madison, Wis
- Rutten R. J., 2003, Radiative Transfer in Stellar Atmospheres
- Seager S., Deming D., 2010, *Annual Review of Astronomy and Astrophysics*, 48, 631
- The JWST Transiting Exoplanet Community Early Release Science Team et al., 2022, Identification of carbon dioxide in an exoplanet atmosphere, [doi:10.48550/ARXIV.2208.11692](https://arxiv.org/abs/2208.11692), <https://arxiv.org/abs/2208.11692>
- Wakeford H. R., et al., 2017, The Astronomical Journal, 155, 29